Tuning of Intermolecular Electron Transfer Reaction by Modulating the Microenvironment Inside Copolymer−Surfactant Supramolecular Assemblies

ARTICLE *in* THE JOURNAL OF PHYSICAL CHEMISTRY B · FEBRUARY 2011

Impact Factor: 3.3 · DOI: 10.1021/jp109217v · Source: PubMed

8 AUTHORS, INCLUDING:

Swayandipta Dey
University of Connecticut
36 PUBLICATIONS **682** CITATIONS
SEE PROFILE

Prabhat Singh
Bhabha Atomic Research Centre
37 PUBLICATIONS **491** CITATIONS
SEE PROFILE

Vinod K Aswal
Bhabha Atomic Research Centre
392 PUBLICATIONS **4,905** CITATIONS
SEE PROFILE

Haridas Pal
Bhabha Atomic Research Centre
193 PUBLICATIONS **4,933** CITATIONS
SEE PROFILE

THE JOURNAL OF PHYSICAL CHEMISTRY B

ARTICLE

pubs.acs.org/JPCB

Tuning of Intermolecular Electron Transfer Reaction by Modulating the Microenvironment Inside Copolymer−Surfactant Supramolecular Assemblies

Manoj Kumbhakar,*[,†] Swayandipta Dey,[⊥] Prabhat Kumar Singh,[†] Sukhendu Nath,[†] Ashis Kumar Satpati,[‡] Rajib Gangully,[§] Vinod Kumar Aswal,[∥] and Haridas Pal[†]

[†]Radiation & Photochemistry Division, [‡]Analytical Chemistry Division, [§]Chemistry Division, and [∥]Solid State Physics Division, Bhabha Atomic Research Centre, Mumbai 400 085, India

[⊥]Chemistry Department, Pondicherry University, Kalapet, Pondicherry 605014, India

ABSTRACT: Photoinduced intermolecular electron transfer (ET) dynamics between various 7-aminocoumarin acceptors and *N*,*N*-dimethylaniline (DMAN) donor has been studied in copolymer−surfactant supramolecular assemblies prepared in aqueous 1% P123 triblock copolymer micellar solution with varying concentration of surfactants (sodium dodecyl sulfate (SDS), cetyl trimethyl ammonium chloride (CTAC), and triton-X-100 (TX100)). The aim of the present study is to modulate the reaction environment, especially the degree of micellar hydration inside the P123 micelle by the addition of the surfactants, which can modulate the ET reaction through the changes in the ET rates and the reaction exergonicity. Within the limited surfactant to copolymer molar ratios (***n***) used in the present study, fluorescence spectroscopy, dynamic light scattering (DLS), and small-angle neutron scattering (SANS) investigations indicate that the copolymer−surfactant supramolecular assemblies retain their micellar structure, although the micellar size gradually decreases with ***n***. The redox potentials of the electron donor and acceptors are also found to change with ***n***, although the extent of the effect is different for SDS, CTAC, and TX100 cosurfactants. In the presence of CTAC, the estimated exergonicity ($-\Delta G^0$) of the ET reaction is found to increase with an increase in ***n*** compared with that in pure P123, whereas it decreases marginally with SDS and remains almost the same for TX100. Substantial quenching of coumarin fluorescence is observed in the presence of DMAN in all copolymer−surfactant micellar aggregates because of ET reaction. The ET rate is seen to increase gradually with an increase in SDS and CTAC concentration in the supramolecular assembly, although it remains unaffected on the addition of TX100. The increased ionic strength in the Corona region of the copolymer−surfactant supramolecular aggregates due to the addition of the ionic surfactants has been envisaged for the increase in the ET rates. A correlation of the quenching rate constants with the free-energy changes (ΔG^0) of the ET reactions shows the typical bell-shaped curve as predicted by Marcus outersphere ET theory. A substantial shift along the exergonicity axis (∼0.3 eV) for the appearance of the Marcus correlation is observed in some cases, although the extent of such shift depends on both the nature of the cosurfactant and the amount of cosurfactant used in the copolymer−surfactant supramolecular assembly. Therefore, these preliminary results suggest a possibility of not only modulating the ET rates but also tuning the appearance of Marcus inversion along the exergonicity scale by suitably tuning the reaction environment inside the copolymer−surfactant supramolecular assemblies with a relatively more hydrophilic cosurfactant.

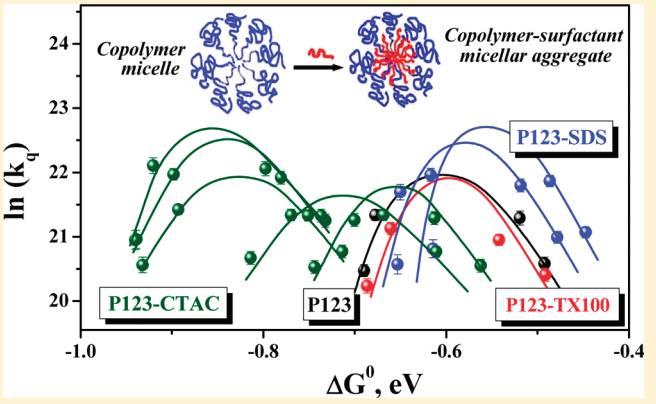

INTRODUCTION

Of late, considerable efforts have been made to explore the details of electron transfer (ET) processes in various organized assemblies to control the dynamics and mechanism of ET reactions.[1−27] Our recent studies on photoinduced ET by selecting micelles as the reaction media (namely, sodium dodecyl sulfate (SDS),[6,10] cetyl pyridinium chloride (CPC),[11] cetyl trimethyl ammonium bromide (CTAB),[8] dodecyl-trimethyl ammonium bromide (DTAB),[8,9] Pluronic P123,[13] Pluronic F88,[15] and triton-X-100 (TX100)[7,12,14]) we tried to modulate the ET parameters in such a way that the bell-shaped Marcus correlation for bimolecular ET reactions can be demonstrated as well as modulated in terms of the ET rates and reaction exergonicity. As a consequence of the entanglement of the reactants with the

Received: September 27, 2010
Revised: December 21, 2010
Published: January 27, 2011

surfactant chains and slower solvent reorganization inside micelles, the unique inversion in the ET rates for bimolecular ET reactions at unexpectedly lower exergonicity (~0.7 eV) has been observed and envisaged by invoking the two-dimensional ET (2DET[28]) model, where reaction occurs mainly through the nuclear vibrational coordinate, as the movement along the solvent coordinate is slower than the ET rates.[10,11] The most notable observation in all of these studies is the modulation of ET dynamics by suitable selection of the micellar media. Depending on the relative propensity of the solvation and the ET rates, a nearly 0.7 eV shift in the exergonicity for the appearance of the Marcus inversion region has been demonstrated between DTAB and SDS micelles.[8,9,11,14] Although, these results are promising, but changing one micelle to another to tune the ET dynamics downplays its credential for any practical utilization. The alternative strategy of tuning ET reactions is to modulate the reactant microenvironment inside the same micelle instead of changing the whole micellar system—the theme of the present research project.

The key factors in tuning the reaction microenvironment inside the micelle for a favorable ET reaction are the degree of hydration (i.e., micropolarity), solvent relaxation (i.e., contribution of solvent reorganization energy depending on the relative propensity of the solvation and the ET rate), and the microviscosity or the surfactant entanglement (i.e., donor—acceptor separation).[9−11,29−32] The first two parameters directly influence the driving force of the ET reaction, whereas the last one determines the reaction rate. The common means of altering the microenvironment inside a micelle is the addition of electrolyte or cosurfactant or changing the temperature or pressure of the system. The addition of electrolyte (like NaCl, KCl, CsCl, etc.) increases the degree of hydration in the micelles[33−40] and is expected to facilitate ET dynamics, but the presence of a high amount of electrolyte in the Corona region will also influence the micellar shape.[35,41−44] Variation in the temperature substantially influences the degree of micellar hydration as well as the solvation dynamics.[45−47] However, change in the temperature of the micellar solution is also not promising because cloud point temperature and solubility of surfactants may limit the practically achievable temperature range with micellar media.[48−50] The application of high pressure to modify the hydration and solvation dynamics in micellar media requires special experimental arrangements.[51−54] Solvation dynamics of C480 become faster with an increase in pressure in TX100 but slows down in SDS micelles.[51−53] Another way of altering the micellar hydration and solvation dynamics is the simple addition of another surfactant (of different hydrophilicity) to the micellar solution, in which the ratio of the two surfactants can be easily varied to alter the microenvironment.[55−57] Block copolymer nanostructures are often used in conjunction with ionic surfactants to modulate their functional properties.[58−60] Because of synergistic interaction among these surfactants,[61−64] their performance improves compared with that of individual components. In view of all these, the addition of surfactant to a triblock copolymer micelle seems much more promising, and we have attempted to carry out a detailed study on the effect of different types of surfactants (ionic and nonionic) on the ET dynamics in a triblock copolymer micelle. Although structural aspects and solvation dynamics in block copolymer—surfactant aggregates have been reported, but to the best of our knowledge, this is the first attempt to study the ET processes in such copolymer—surfactant supramolecular assemblies to modulate the energetics and dynamics of the ET reactions.

Chart 1. Schematic for Copolymer and Copolymer—Surfactant Aggregates (Micelles) at Low Surfactant-to-Copolymer Ratios (*n*)

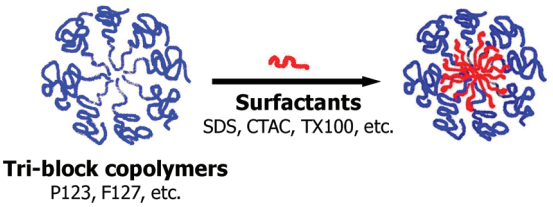

In this report, we present the ET results between coumarin derivatives and *N*,*N*-dimethylaniline (DMAN) in aqueous triblock copolymer EO_{20}-PO_{70}-EO_{20} (P123; EO: ethylene oxide and PO: propylene oxide) micellar media with the gradual addition of cationic, anionic, and neutral surfactants (cetyltrimethyl ammonium chloride (CTAC), SDS, and TX100, respectively) at a fixed P123 concentration of 1% w/v. Above a certain temperature, the poly-PO block turns hydrophobic, and consequently, the triblock copolymers (henceforth we will refer as copolymers) exhibit amphiphilic character to form micelles in aqueous solutions.[49] It is reported in the literature that in the presence of a low concentration of cosurfactants, the copolymer micelles form unique copolymer—surfactant supramolecular aggregates.[57,63−75] In these copolymer-rich mixed aggregates, it has been proposed that the nonpolar tail of the added surfactants resides in the core of the micelle composed of PO units, and the polar head groups of the surfactants tend to protrude from the core into the Corona layer composed of EO units (cf. Chart 1).[57,72,73]

Investigations by Jansson et al.[72,73] reveal that in the region of low surfactant-to-copolymer ratio (*n*), the copolymer micelles are associated with few ionic surfactants (SDS and CTAC). In contrast, at high *n* region (>10), copolymer-rich aggregates are disrupted and small surfactant-rich micelles with few attached copolymer molecules are formed. However, there is a difference in opinion regarding the nature of the copolymer—surfactant aggregates in the intermediate *n* region (~2—9). According to Jansson et al., during the transformation of copolymer-rich micelles ($n < 2$) to surfactant-rich micelles ($n > 10$) both copolymer-rich and surfactant-rich aggregates coexist,[72,73] whereas SANS studies by Ganguly et al.[57] indicate the presence of only one type of micellar aggregates. Later, it has been observed from fluorescence spectroscopic investigations that in the intermediate *n* region the transformation of a dominantly copolymer-rich complex to a mainly surfactant-rich complex, depending on the copolymer concentration can occur either by gradual incorporation of surfactants into the copolymer-rich micelles with concomitant release of copolymer units until surfactant-rich micelles are formed or by simultaneous buildup of surfactant-rich micelles together with the destruction of copolymer-rich micelles.[55] However, to avoid any complicacy related to the nature and identity of the copolymer—surfactant aggregates, in the present study, we will limit ourselves only to the low *n* (<3 at a fixed 1% P123 concentration) region of the ionic surfactants (SDS and CTAC) in the P123 micellar solution. Recent light scattering and calorimetry studies of P123 in the presence of nonionic surfactant $C_{12}EO_6$ by Löf et al.[64,76,77] also report the formation of mixed micelles. Moreover, at elevated temperatures, a well-defined shape

transition of these micelles from spherical to rod-like shape is also noticed.[77] At $C_{12}EO_6$/P123 molar ratios in the range of 2 to 3, all mixed aggregates are in the form of spheres at temperatures below 38 °C (lower critical solution temperature (LCST)) and in the form of rods above 46 °C. For all other molar ratios (up to 46), LCST is well above 40 °C. Cryotransmission electron microscopy of aqueous mixtures of a nonionic surfactant $C_{12}EO_5$ and block copolymers are also reported.[78] In the present study, we have used nonionic surfactant TX100 (instead of $C_{12}EO_{16}$) to form mixed aggregates. Following similarity of $C_{12}EO_6$ and TX100, it is assumed that in the present experimental condition (at ambient temperature, 25 °C and $n \leq 8$), mixed aggregates are spherical in shape and transition to rod-like shape is neglected. However, systematic characterization of micellar parameters by small-angle neutron scattering (SANS) and by dynamic light scattering (DLS) of all of these copolymer−surfactant systems has been carried out independently in the present study.

ET reactant pairs, that is, coumarins and amine, preferentially reside in the Corona region of P123 micelles, with dielectric constant (ε) around 10.[13] Because the degree of hydration in the Corona region of TX100 micelle ($\varepsilon \approx 26$[7]) is considerably greater than that of P123, an increase in the hydration in the Corona region of P123 micelle is expected with the gradual incorporation of TX100 in it. This increase in hydration will facilitate ET reaction in P123−TX100 aggregates compared with that in P123 micelles.[29] Similar argument also holds for the addition of anionic surfactant SDS ($\varepsilon \approx 40$ for the Stern layer of SDS micelle[10]) and cationic surfactant CTAC ($\varepsilon \approx 40$ for similar Stern layer of CTAB micelle[8]) to P123 micelles. Besides, we have selected nonionic surfactant TX100 and ionic surfactants SDS and CTAC mainly to compare the influence of ionic nature of the surfactant head groups on the ET dynamics in P123−surfactant supramolecular aggregates.

METHODS

The copolymer, P123, was obtained from Aldrich and used without further purification. SDS, CTAC, and TX100 samples were obtained from Sigma, Aldrich, and Riedel-de Haën, respectively, and used as received. Laser-grade coumarin dyes (coumarin-153 (C153), coumarin-152 (C152), coumarin-481 (C481), coumarin-151 (C151)) were obtained from Exciton and used as received. *N*,*N*-Dimethylaniline (DMAN) was obtained from Spectrochem, India and were purified by vacuum distillation just before use. The chemical structures of the acceptors (coumarin dyes) and the donor (DMAN) used in this study are given in Chart 2. Nanopure water, having a conductivity of <0.1 μS cm^{-1}, was obtained by using a Millipore Gradiant A10 system and used for the preparation of the micellar solutions.

In the experimental solutions, the concentration of P123 was kept 1% w/v (1.75 mM). A P123 stock solution of 5% w/v was prepared first, by weighing the required amount of block copolymer and kept overnight under refrigeration after the addition of a requisite amount of water in a sealed container. The solutions of P123−surfactant (solution 1; P123−SDS, P123−CTAC, and P123−TX100 with P123 and surfactant concentrations of 1.75 and 50 mM, respectively) were prepared by mixing the requisite amount of 5% P123 stock, surfactant, and water. Only P123 solution of 1.75 mM (solution 2; 1.75 mM) was also prepared from the 5% P123 stock solution by dilution. In these experiments, different molar ratios (n) of surfactant to P123 were prepared by proportional mixing of solution 2 (only P123) and solution 1 (P123−surfactant), thereby keeping the copolymer concentration constant. Samples were prepared by adding coumarins in the aqueous solution of P123−surfactants at room temperature. The concentration of the dyes (~1 μM) was kept much lower in comparison with the micelle concentration (~20 μM).[13] With the above experimental condition, only a small fraction of the micelles can have a dye molecule in them, and the number of micelles having more than one dye molecules inside is negligible.[48]

Chart 2. Chemical Structures of the Coumarin Acceptors and the DMAN Donor

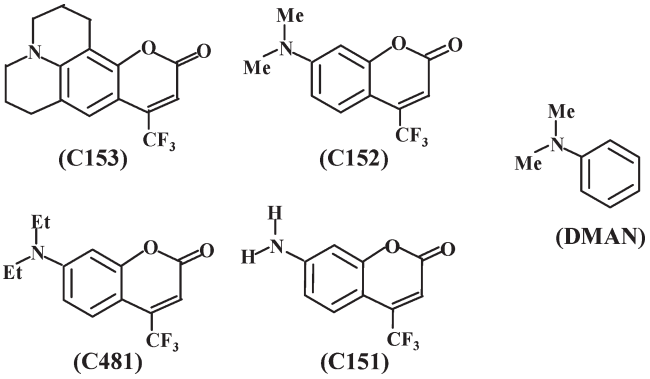

Fluorescence Spectroscopy. Ground-state absorption and steady-state (SS) fluorescence spectra were recorded using a Shimadzu (Tokyo, Japan) model UV-160A UV−vis spectrophotometer and Hitachi (Tokyo, Japan) model F-4500 spectrofluorimeter, respectively. Time-resolved (TR) fluorescence measurements were carried out using a diode-laser-based subnanosecond fluorescence spectrometer from IBH, U.K. (Glasgow). The instrument works on the principle of time-correlated single photon counting (TCSPC[79]). In the present work, a 374 nm diode laser (<100 ps, 1 MHz) was used as the excitation source, and a MCP PMT-based detector (IBH) was used for fluorescence detection. The instrument response function for the present setup is ~130 ps at fwhm. For lifetime measurements, fluorescence decays were recorded at magic angle (54.7°) with respect to the vertically polarized excitation light. All experiments were carried out at ambient temperature, 25 ± 1 °C. Fluorescence anisotropy measurements were carried out by measuring the fluorescence decays with parallel, $I_{II}(t)$, and perpendicular, $I_{\perp}(t)$, polarizations using vertically polarized excitation beam. The anisotropy decay function $r(t)$ was constructed using the following relation[30]

$$r(t) = \frac{I_{II}(t) - GI_{\perp}(t)}{I_{II}(t) + 2GI_{\perp}(t)} \quad (1)$$

where G is a correction factor for the polarization bias of the detection system. The G factor was independently obtained by using the horizontally polarized excitation beam and measuring the two perpendicularly polarized fluorescence decays. For anisotropy measurements, fluorescence decays were collected with a larger spectral bandwidth of ~16 nm, to avoid the influence of solvent relaxation on the anisotropy decays. Measurements were repeated three times, both to check the reproducibility and to obtain the average values of the decay parameters.

Redox Potential Measurements. Reduction potentials of the coumarin dyes [$E(C/C^-)$] in P123 and P123−surfactant micellar aggregate solutions were measured by cyclic voltammetric (CV) method using Eco Chemie Potentiostat/Galvanostat-20 and GPES software. Solutions of the coumarin dyes in micellar media containing 0.01 mol dm^{-3} potassium chloride as the supporting electrolyte were first deaerated by purging high purity N_2 gas for ∼10 min. CV measurements were then carried out using hanging mercury drop as the working electrode, graphite rod as the counter electrode, and saturated calomel electrode (SCE) as the reference electrode. The oxidation potentials of DMAN ($E(A/A^+)$) in P123 and P123−surfactant micellar aggregates were also estimated by CV measurements using glassy carbon (GC) as the working electrode. All redox potentials listed in Tables 1−3 are against SCE.

Table 1. Various Energy Parameters for ET Reaction between Coumarin and DMAN in 1% w/v Solution of P123 and at Different Molar Ratios of TX100 to P123 (n)

n	dye	$E(C/C^-)$, V	E_{00} (dye), eV	$E(A/A^+)$, V	τ_0, ns	ΔG^0, eV	k_q, 10^8 M^{-1} s^{-1}
0	C153	−1.58	2.68	0.81	5.36	−0.492	8.70
	C481	−1.67	2.79		4.09	−0.520	17.69
	C152	−1.54	2.81		4.24	−0.677	18.53
	C151	−1.57	2.85		5.92	−0.690	7.79
2	C153	−1.56	2.67	0.83	5.36	−0.493	8.65
	C481	−1.65	2.80		4.15	−0.522	15.64
	C152	−1.52	2.81		4.15	−0.672	18.29
	C151	−1.54	2.84		6.02	−0.689	7.98
4	C153	−1.54	2.67	0.85	5.08	−0.484	8.04
	C481	−1.63	2.80		3.69	−0.527	15.65
	C152	−1.52	2.81		3.69	−0.658	15.72
	C151	−1.54	2.84		5.68	−0.668	6.83
8	C153	−1.53	2.67	0.85	4.96	−0.491	7.55
	C481	−1.62	2.80		3.78	−0.542	12.98
	C152	−1.52	2.81		3.63	−0.661	15.51
	C151	−1.52	2.84		5.90	−0.686	6.34

Estimation of Free Energy Changes. In the present coumarin−amine systems, the values for the free energy changes (ΔG^0) for the ET reactions were calculated using the following relation[80]

$$\Delta G^0 = E_{A/A^+} - E_{C/C^-} - E_{00} - \frac{e^2}{\varepsilon R_0} \quad (2)$$

where E_{00} is the excitation energy of the coumarins from the S_0 state to the S_1 state, e is the charge of an electron, ε is the static dielectric constant of the micellar microenvironment, and R_0 is the center-to-center distance between the interacting coumarin and DMAN. E_{00} values of the coumarins were obtained from the intersecting wavelengths of the normalized (peak intensities) fluorescence and excitation spectra and are listed in Tables 1−3. The radii of the DMAN donor and coumarin acceptors were estimated using Edward's volume addition method, and R_0 was considered to be equal to the sum of the radii of the DMAN and the coumarin involved. The ε values in the corona regions were considered to be ∼10 for all P123−surfactant micellar

Table 2. Various Energy Parameters for ET Reaction between Coumarin and DMAN in 1% w/v Solution of P123 and at Different Molar Ratios of CTAC to P123 (n)

n	dye	$E(C/C^-)$, V	E_{00}(dye), eV	$E(A/A^+)$, V	τ_0, ns	ΔG^0, eV	k_q, 10^8 M^{-1} s^{-1}
0.01	C153	−1.49	2.67	0.82	5.75	−0.562	9.95
	C481	−1.58	2.81		3.93	−0.613	20.79
	C152	−1.50	2.82		4.32	−0.700	20.19
	C151	−1.50	2.86		5.98	−0.744	9.71
0.05	C153	−1.42	2.66	0.84	5.71	−0.611	8.88
	C481	−1.51	2.81		4.25	−0.669	15.73
	C152	−1.43	2.82		4.43	−0.751	15.61
	C151	−1.42	2.87		5.98	−0.814	8.06
0.5	C153	−1.26	2.67	0.90	5.63	−0.714	10.49
	C481	−1.35	2.81		4.16	−0.770	18.49
	C152	−1.23	2.81		4.19	−0.893	20.20
	C151	−1.25	2.88		5.91	−0.932	8.52
1	C153	−1.22	2.66	0.91	5.36	−0.732	16.99
	C481	−1.32	2.81		4.02	−0.781	33.14
	C152	−1.21	2.81		4.02	−0.898	34.89
	C151	−1.23	2.87		5.91	−0.939	12.69
2	C153	−1.21	2.65	0.91	5.30	−0.737	18.33
	C481	−1.30	2.81		4.06	−0.798	38.16
	C152	−1.18	2.81		3.98	−0.921	39.98
	C151	−1.22	2.87		4.87	−0.940	12.55

dx.doi.org/10.1021/jp109217v |J. Phys. Chem. B 2011, 115, 1638–1651

Table 3. Various Energy Parameters for ET Reaction between Coumarin and DMAN in 1% w/v Solution of P123 and at Different Molar Ratios of SDS to P123 (n)

n	dye	$E(C/C^-)$, V	E_{00} (dye), eV	$E(A/A^+)$, V	τ_0, ns	ΔG^0, eV	k_q, 10^8 M^{-1} s^{-1}
0.5	C153	−1.58	2.66	0.82	5.17	−0.468	12.83
	C481	−1.68	2.80		3.70	−0.504	23.79
	C152	−1.55	2.81		3.82	−0.645	23.59
	C151	−1.58	2.84		5.59	−0.652	9.01
1	C153	−1.58	2.66	0.81	5.08	−0.478	13.07
	C481	−1.67	2.80		3.81	−0.519	29.27
	C152	−1.55	2.80		3.86	−0.650	26.48
	C151	−1.58	2.84		5.66	−0.653	8.60
2	C153	−1.57	2.66	0.84	4.79	−0.447	14.16
	C481	−1.67	2.79		3.56	−0.487	31.44
	C152	−1.54	2.79		3.46	−0.617	34.67
	C151	−1.58	2.83		5.81	−0.615	10.96

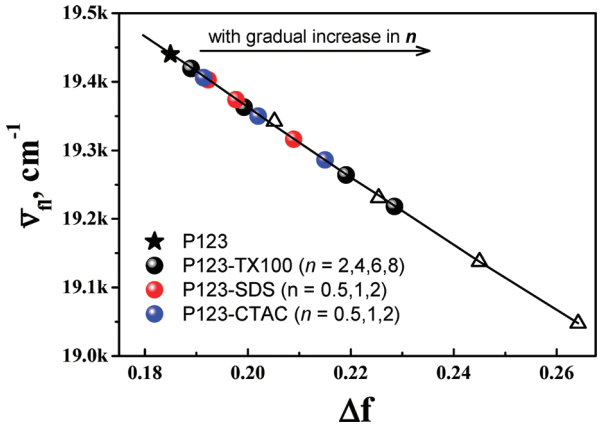

Figure 1. Plot of fluorescence maxima ($\bar{\nu}_{fl}$, in cm^{-1}) of C153 against the solvent polarity function (Δf) for different monoalcoholic solvents (Δ). An emission maximum shows small gradual red shift with increase in surfactant-to-copolymer ratio (n). Data points corresponding to the C153 emission maxima in P123 (star), P123−SDS (red spheres), P123−CTAC (blue spheres) and P123−TX100 (black spheres) micellar systems at different n values are indicated.

aggregates,[13] although their effect on $\Delta G°$ via the Coulomb interaction term is quite low. However, to have a quantitative estimate for the polarity (ε) of the microenvironment around the probe in P123−surfactant aggregates, the fluorescence spectra of the C153 dye were recorded in different alcohol solvents (decanol, octanol, hexanol, butanol, etc.) to obtain a calibration curve by plotting the emission maxima ($\bar{\nu}_{fl}$) in these solvents against the solvent polarity function, Δf, defined as[13,30,81]

$$\Delta f = \frac{\varepsilon - 1}{2\varepsilon + 1} - \frac{n_r^2 - 1}{2n_r^2 - 1} \quad (3)$$

where ε is the static dielectric constant and n_r is the refractive index of the solvent. For pure solvents, ε and n_r values were obtained from the literature. The typical calibration curve thus obtained is shown in Figure 1, which is linear within the experimental error. Using this calibration curve and noting the fluorescence maxima of the C153 dye in the micelles, the ε values for the localization sites of the dye in different P123−surfactant aggregates were estimated to be in the range of 7−12 (assuming the n_r similar to that of decanol). The ΔG^0 values estimated for different coumarin−DMAN pairs in all the three P123−surfactant micellar aggregates are listed in Tables 1−3.

Dynamic Light Scattering Studies. DLS measurements of the solutions were performed using a Malvern 4800 Autosizer employing 7132 digital correlator. The light source was a He−Ne laser operated at 633 nm with a maximum output power of 25 mW, and the scattered light was detected by an avalanche photodiode (APD). The average decay rates (Γ) of the electric field autocorrelation functions, $g^1(\tau)$, were obtained by using the method of cumulants.[82,83] Diffusion coefficients (D) of the scattering particles were calculated using the following equation:

$$\Gamma = Dq^2 \quad (4)$$

where q is the magnitude of the scattering vector given by $q = [4\pi n_r \sin(\theta/2)]/\lambda$, where n_r is the refractive index of the solvent, λ is the wavelength of laser light, and θ is the scattering angle. Γ versus q^2 plots were generated by carrying out measurements at five different angles ranging from 50 to 130°. For the diffusive scattering species, these Γ versus q^2 plots are linear, and the diffusion coefficients were calculated from the observed slopes. The hydrodynamic radius, R_M of the scattering particles was calculated using the Stokes−Einstein equation.

$$R_M = \frac{kT}{6\pi\eta D} \quad (5)$$

where k is the Boltzmann constant, T is the absolute temperature, and η is the viscosity of the medium.

Small-Angle Neutron Scattering. Neutron scattering measurements were carried out using the facility at the Dhruva reactor, Trombay, India.[84] The mean incident wavelength (λ) of the neutron was 5.2 Å with resolution $\Delta\lambda/\lambda$ about 15%. The scattered neutrons were measured using a 1D position-sensitive detector for the scattering vector (Q) range of 0.017−0.35 $Å^{-1}$. The measured SANS data were corrected for the background, the empty cell contribution, and the transmission and were presented on an absolute scale using the standard protocols. All SANS measurements were carried out in D_2O

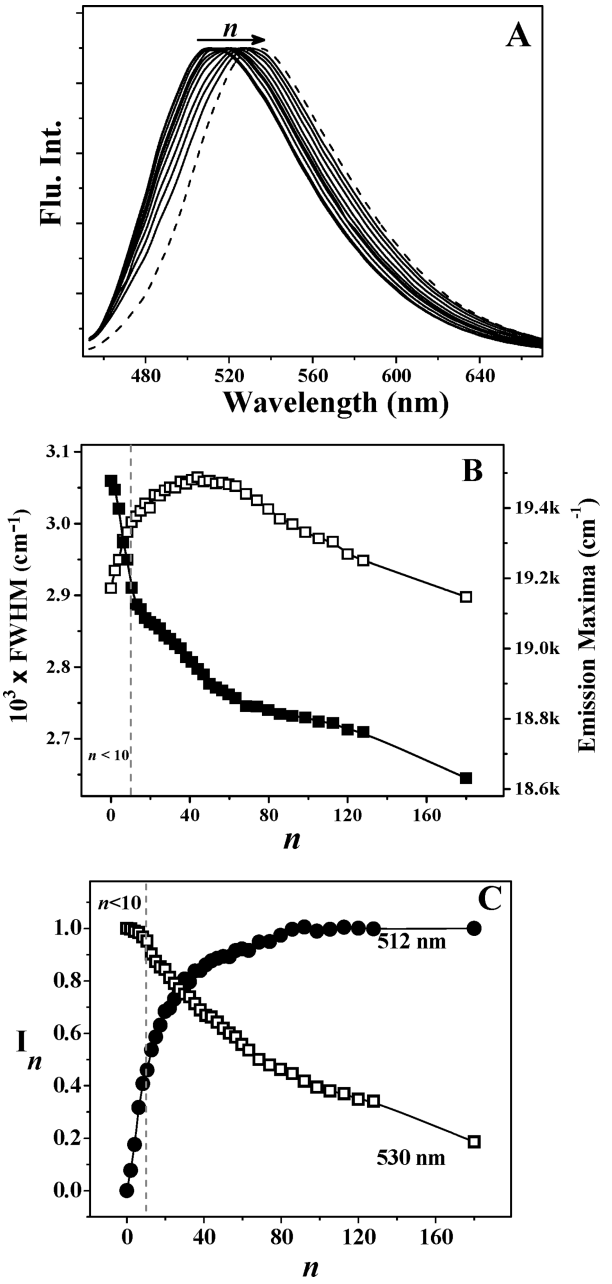

Figure 2. (A) Normalized fluorescence spectra of C153 at different n values (0, 2.0, 6.2, 10.5, 12.8, 17.4, 27.3, 50.0, 68.6, 127.9) for P123−TX100 system at constant P123 concentration of 1 % w/v. Fluorescence spectrum of C153 in TX100 micelles is indicated by the dashed spectra. (B) Plot of fwhm (-□-) and emission maxima (-■-) of C153 as a function of n. (C) Plot of I_n as a function of n at two different emission wavelengths, 512 (for copolymer rich aggregates) and 530 nm (for copolymer rich aggregates).

solvent because of the better contrast for micelles in D_2O than in H_2O.

In SANS experiments, one measures the coherent differential scattering cross-section per unit volume ($d\Sigma/d\Omega$) as a function of Q. In the case of monodispersed particles dispersed in a medium, it can be written as[85]

$$\frac{d\Sigma}{d\Omega}(Q) = nV^2(\rho_p - \rho_s)^2 P(Q)S(Q) + B \qquad (6)$$

where n is the number density and V is particle volume. ρ_p and ρ_s are scattering length densities of particles and solvent, respectively. $P(Q)$ is the intraparticle structure factor and depends on the shape and size of the particles. $S(Q)$ is the interparticle structure factor decided by the interaction between particles and is unity for dilute systems. B is a constant term representing incoherent background.

For polydispersed systems, $d\Sigma/d\Omega$ in eq 1 is modified as[86]

$$\frac{d\Sigma}{d\Omega}(Q) = \int \frac{d\Sigma}{d\Omega}(Q,R) f(R)\, dR + B \qquad (7)$$

where $f(R)$ is the size distribution and usually accounted by the log-normal distribution.

All SANS data have been fitted using the polydispersed spherical mixed micelles of P123−surfactant systems. The scattering from the shell region of the micelles is neglected because of the poor contrast of this hydrated part as compared with that of the core. The parameters in the analysis were optimized by means of nonlinear least-squares fitting program. Correction due to the instrumental smearing was also taken into account throughout the data analysis.

RESULTS AND DISCUSSION

Steady-state fluorescence measurements were carried out to study the aggregation behavior of TX100 with P123 micelles employing C153 as the fluorescence probe. Similar studies with SDS and CTAC are well reported in the literature.[55] Gradual increase in TX100 concentration at a fixed P123 concentration (of 1% w/v) leads to spectral shift toward lower energy, quite similar to that observed with SDS and CTAC, along with the changes in fwhm and normalized spectral intensity (I_n). Three different regions for P123−TX100 aggregates are also evident from the alteration pattern of emission maxima, fwhm, and I_n at different n values, as shown in Figure 2. However a close look at these parameters clearly suggests that interaction of TX100 is largely inept to alter the properties of P123 assemblies compared with other surfactants, SDS and CTAC.[55] This is probably due to the physicochemical behavior of TX100 that is akin to P123, because both of them consist of polyethylene oxide that constitutes the Corona region. On the contrary, the ionic head groups of SDS and CTAC, which are heavily hydrated, result in much larger alteration of the micellar characteristics once they are incorporated into P123 assemblies. In corroboration with the previous results of P123−SDS and P123−CTAC systems, it is evident from Figure 2 that P123−TX100 aggregates exist until $n \approx 80$, a value distinctly higher than that observed with SDS and CTAC ($n \approx 10$, above which only surfactant rich aggregates exist[55]). Additionally, destruction of P123 rich-aggregates starts at reasonably higher n values (∼10) than those observed with SDS or CTAC (∼3[55]). To be noted, the aggregation of TX100 with P123 requires further investigation to confirm the proposed mechanism, although from the similarity of this system with that of P123−SDS/CTAC, a single P123−TX100 micellar aggregate can be envisaged in the $n < 10$ region. This also corroborates well with the findings of DLS and SANS results, discussed later. Hence, to avoid any complicacy related to the nature and identity of the copolymer−surfactant aggregates, in the present study, to use such systems as the ET reaction media, we limit ourselves only to the low n region (at a fixed 1% P123 concentration) of <3 for SDS and CTAC and <10 for TX100.

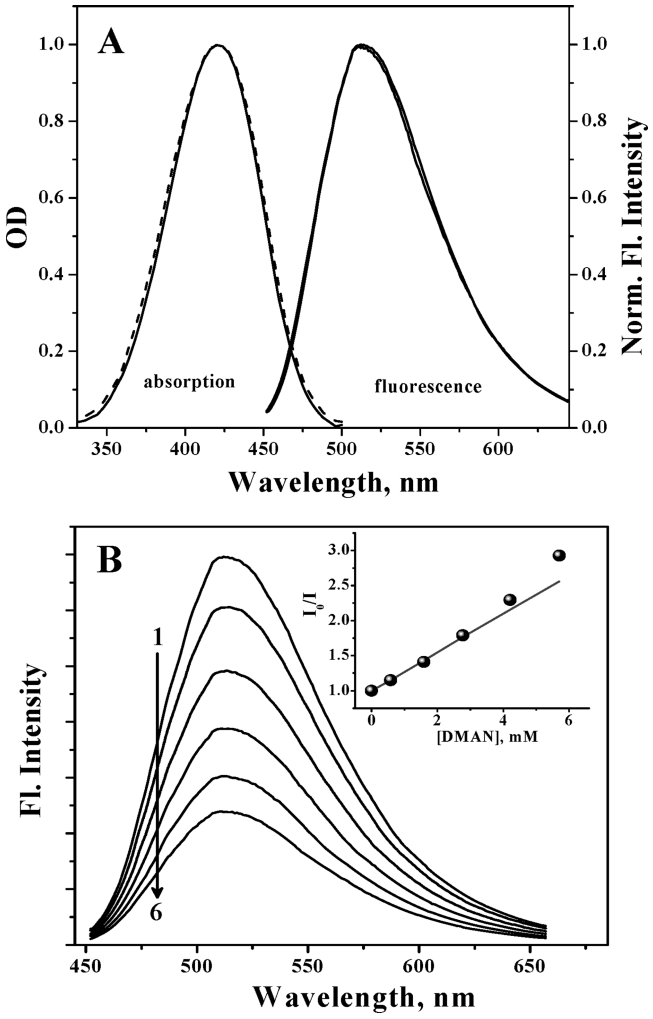

Figure 3. (A) Absorption and fluorescence spectra of C153 in the absence (solid line) and the presence of 5.7 mM DMAN (dashed line) in P123−TX100 (n = 2) aggregates. Fluorescence spectra are plotted after peak normalization. (B) Fluorescence quenching of C153 with increasing concentration of DMAN in P123−TX100 (n = 2) aggregates. The spectra 1 to 6 are at DMAN concentrations of 0, 0.6, 1.6, 2.8, 4.2, and 5.7 mM. Inset shows the corresponding SV plot obtained from the SS measurements.

The solubility of both the coumarins and DMAN in water is very low, but in the presence of micelles (P123, SDS, CTAC, TX100, etc.) or mixed micellar aggregates, their solubility increases substantially.[6−12,32,55,56,87] According to the literature reports, these molecules reside preferentially inside the Corona region of the micelles. Coumarin fluorescence spectra were observed to show marginal red shift with the gradual addition of surfactants in P123 micellar solution (cf. Figures 1 and 2), known to be due to the increased hydration and micropolarity ($\Delta\varepsilon \approx 5$, cf. Figure 1).[55,56] From SS measurements, it is seen that the fluorescence intensity of the coumarin dyes in all P123−surfactant micellar aggregates is quenched by the addition of DMAN in the solution. Typical absorption and fluorescence spectra of C153 in P123−TX100 aggregates of n = 2 composition in the absence and presence of different concentrations of DMAN are shown in Figure 3. It is indicated from Figure 3B that although the fluorescence intensity of the dye is reduced substantially in the presence of the amine quencher, the shape

Table 4. Fitted Micellar Parameter of Copolymer−surfactant Supramolecular Aggregates Obtained from SANS and DLS Studies[a]

		SANS results				DLS results
systems	n	R_C, nm	polydispersity	N_{P123}	$N_{surfactant}$	R_M, nm
P123−TX100	0	5.33	0.24	94	0	9.30
	2	4.69	0.22	58	116	8.30
	4	4.16	0.22	37	148	7.00
	8	3.51	0.22	19	152	5.70
P123−CTAC	0.01	5.27	0.24	91	1	9.30
	0.05	4.87	0.24	72	4	9.00
	0.5	4.74	0.24	66	33	8.35
	1	4.23	0.23	43	43	8.15
	2	4.10	0.22	37	74	7.65
P123−SDS	0.5	4.98	0.23	74	37	8.35
	1	4.72	0.23	62	62	7.90
	2	4.33	0.22	46	92	7.40

[a] R_C: micellar core radius; N_x: number of x units in P123−surfactant aggregates; R_M: micellar hydrodynamic radius.

of the fluorescence spectra does not change, even in the presence of the highest concentration of the amine used (cf. Figure 3A). Similar results were also obtained for the other coumarin-amine systems in all P123−surfactant micellar aggregates. These results thus indicate that there is no exciplex formation during the interaction of the excited coumarin dyes with the amine quenchers.[30] From the ground-state absorption studies also it is observed that the absorption spectra of the coumarin dyes remain unchanged, even in the presence of the highest concentration of the amines used (cf. Figure 3A). It is thus indicated that there is no ground-state complex formation between the coumarin dyes and the amine donors in all P123−surfactant micellar media used in the present study.[30]

To have an estimate of the quenching process in the present systems, SS fluorescence quenching results were correlated following Stern−Volmer (SV) relationship[30,88]

$$\frac{I_0}{I} = 1 + K_{SV}[Q]_{eff} \qquad (8)$$

where I_0 and I are the fluorescence intensities for the coumarin dyes in the absence and presence of the quencher ($Q \equiv$ DMAN), respectively, K_{SV} is the SV constant, and $[Q]_{eff}$ is the effective concentration of the amine quencher in the micellar Corona layer. Because almost all of the DMAN molecules resides in the micellar Corona layer, the effective amine concentration in this region was estimated on the basis of the following considerations. At P123 concentrations used in the present work, effectively spherical micelles are formed.[89] The average diameter of these micelles is estimated to be ∼186 Å, with the nonpolar core diameter of ∼107 Å (cf. Table 4). Therefore, the thickness of the micellar Corona layer is taken to be ∼40 Å, which gives the volume of the micellar Corona layer to be $\sim 2.74 \times 10^4$ Å^3 per micelle or 1647 dm^3 per mole of the micelle ($V_{corona\ layer}$). Considering such a volume and assuming that all amine molecules reside in the micellar Corona layer,

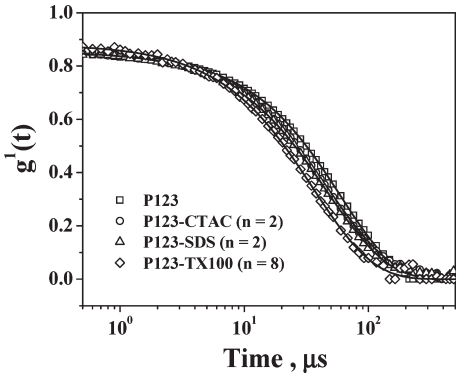

Figure 4. DLS data for the different P123−surfactant micellar aggregates at different ***n*** values. For P123−ionic surfactants, the data were recorded in the presence of 0.1 M NaCl to screen effectively the electrostatic repulsion between the mixed micelles. Solid lines represent the corresponding fits.

the effective amine concentration in the micellar Corona layer is estimated as[10]

$$[Q]_{\text{eff}} = \frac{N_{\text{ag}}[Q]_t}{V_{\text{corona layer}}\{[\text{P123}]_t - \text{CMC}\}} \qquad (9)$$

where N_{ag} is the average aggregation number for P123 micelle ($N_{\text{ag}} \approx 94$), $[\text{P123}]_t$ is the total P123 concentration used (1.75×10^{-3} mol dm^{-3}), CMC is the critical micellar concentration of P123 micelle at ~278 K (~52×10^{-6} mol dm^{-3}), and $[Q]_t$ is the total DMAN concentration used in the solution. The micellar radii of different P123−surfactant aggregates at different ***n*** values have been measured by DLS and that of core by SANS measurements and are shown in Figures 4 and 5. For both of the techniques, the analysis of the data could be done on the basis of the presence of only micelles or mixed micelles as the scattering species with no noticeable presence of any other. As shown in the Figure 4, a decrease in the size of the P123 micelles in the presence of different surfactants is reflected in the shift in the correlation function data toward the lower time scale. In the presence of charged surfactants, the data were recorded in the presence of 0.1 M NaCl to screen effectively the electrostatic repulsion between the mixed micelles.[72,73] The hard sphere radius of the micelles could not be obtained from the SANS data analysis because all measurements were carried out on dilute solutions (1%), and the interparticle structure factor is taken as unity. In view of the fact that the pluronic and SDS are known to show synergistic interaction to form mixed micelles, SANS data analysis were carried out assuming complete association between the P123 and surfactant molecules.[61,62] The micellar parameters obtained from the DLS and the SANS analysis are listed in Table 4. It can be observed that both the micellar radius as well as the core radius decrease gradually with the addition of surfactants, which is shown in the insets of Figure 5. Similar decrease in the copolymer micellar size due to the disintegration of the monomer units with the gradual addition of surfactant is well reported in the literature.[61,72−75]

It is also reported in the literature that in the presence of surfactants, because of the synergistic interaction, pluronics form micelle at lower concentrations than CMC.[61,67,90] The CMC values of the present P123−surfactant mixed systems are not available. However, because the copolymer concentration used (1.75 mM) is much higher than the CMC value of pure P123

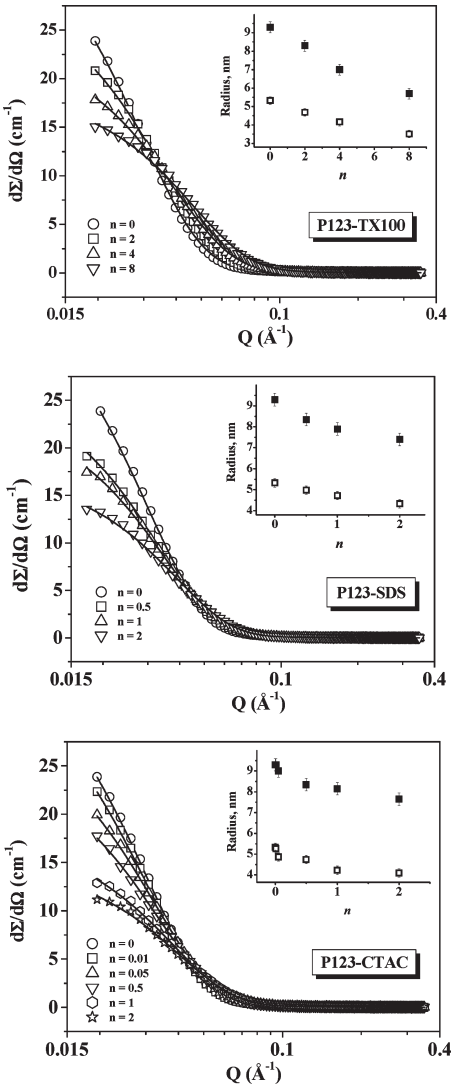

Figure 5. SANS data of the P123−surfactant micellar aggregates at different ***n*** values. Solid lines represent the corresponding fits. Inset shows the variation in the micellar radius (■) and the core radius (□) of different P123−surfactant aggregates at different ***n*** values, estimated from DLS and SANS measurements, respectively.

systems (~0.05 mM at 298 K[49]), we neglect the effect of the change in the CMC value, if any, in our $[Q]_{\text{eff}}$ calculation because no significant change in the estimated concentration values are expected.

Typical I_0/I versus $[Q]_{\text{eff}}$ plot (SV plot) for the C153-DMAN system, as obtained from the SS fluorescence quenching measurements, is shown in the inset of Figure 3B. Similar plots were obtained for other coumarin−DMAN systems. It is to be noted that SV plots from SS quenching show a positive deviation from linearity. In the absence of any ground-state complex formation between the coumarin dyes and the amine quencher, the positive deviations in SV plot seem to be arising because of the higher local concentration of the amine quenchers in the micellar Corona layer, which causes some static quenching for the coumarin−amine pairs that are in close contact.[6−10] Such coumarin dyes thus undergo instantaneous quenching on excitation by the amine molecules in close contact, resulting in a positive deviation from the SV linearity.[30]

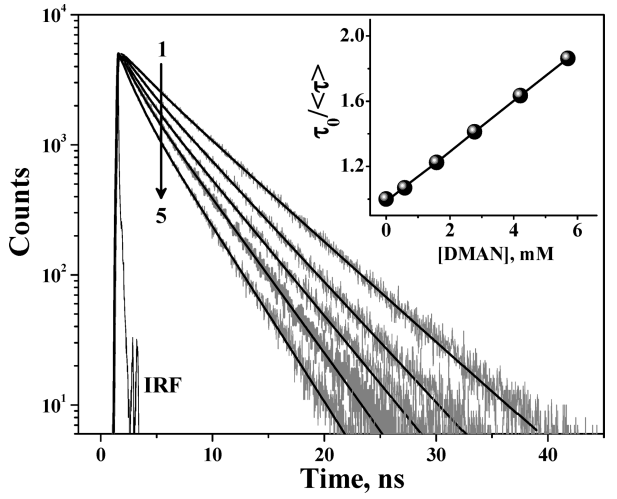

Figure 6. Fluorescence decay traces of C153 in the presence of different concentrations of DMAN in P123−TX100 (n = 2) aggregates. The traces 1 to 5 are at DMAN concentrations of 0, 1.6, 2.8, 4.2, and 5.7 mM. Inset shows the corresponding SV plot obtained from the TR measurements.

The fluorescence decays of the coumarin dyes in P123−surfactant micellar aggregates were measured in the presence of different concentrations of amine to understand the dynamics of interaction in the present systems. It is seen that the fluorescence decays of the dyes gradually become faster as the amine concentration is increased in the solution (cf. Figure 6). In the absence of the amine, the fluorescence decays for all coumarin dyes are seen to fit well with a single-exponential function. The fluorescence lifetimes (τ_0) for coumarin dyes thus estimated in P123−surfactant micellar solutions in the absence of the quenchers are listed in Tables 1−3. In the presence of the amine quencher, the fluorescence decays are seen to become non-single-exponential. To correlate the interaction strengths of different coumarin-amine systems, the average fluorescence lifetime of the coumarin dyes has been considered in such cases, estimated by using the biexponential fitting parameters of the decays.[6−8,10]

To have an estimate of the quenching constant, the reduction in the average fluorescence lifetime (τ) of the coumarin dyes in the micellar media with the effective amine concentrations were correlated following SV relationship (eq 10).[30] Interestingly, it is seen that unlike the case of SS quenching, τ_0/τ versus $[Q]_{eff}$ plots obtained from TR quenching measurements follow the linear SV relation.[6−8,10]

$$\frac{\tau_0}{\tau} = 1 + K_{SV}[Q]_{eff} = 1 + k_q\tau_0[Q]_{eff} \qquad (10)$$

The typical τ_0/τ versus $[Q]_{eff}$ plot for the C153-DMAN system obtained in TR quenching measurements is shown in Figure 6. The k_q values obtained from the slopes of the linear τ_0/τ versus $[Q]_{eff}$ plots for different coumarin−amine systems are listed in Tables 1−3. It is to be noted that for any particular coumarin−amine system, the k_q values obtained from TR measurements are always lower than those obtained from SS measurements (from the initial slope of the SV plots). The apparently higher k_q values obtained from the SS measurements are obviously due to the contribution from the static quenching, which do not contribute in the measured τ values because the fluorescence decays are measured with a subnanosecond TR

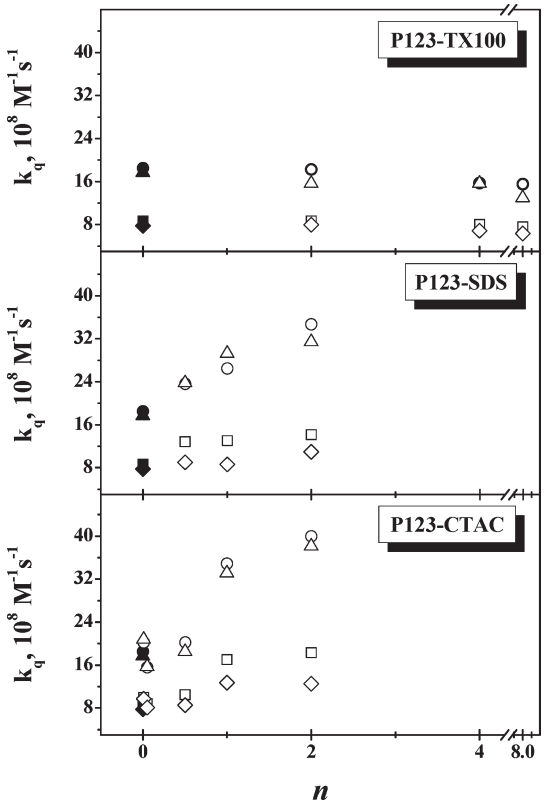

Figure 7. Plot of k_q values for all coumarin dyes (C153 (□), C481 (△), C152 (○), and C151 (◇)) as a function of surfactant-to-copolymer molar ratio, n. The solid symbols represent the k_q values in pure P123 micelles.

instrument (TCSPC).[7,10] Therefore, we infer that k_q values obtained from TR measurements represent the interaction kinetics arising because of the dynamic quenching of the excited dye molecules with the amine quenchers in the micellar Corona layer. In further analysis of our quenching results we will be dealing only with the k_q values obtained from TR measurements.

A comparison of k_q values with the concentration of the added surfactant in P123 micelle indicates an increase in the values for all coumarin−DMAN systems with an increase in n except for TX100, shown in Figure 7. In the presence of CTAC, the k_q value of C153 and C151 increases by a factor of about 2.1 and 1.6, respectively, at n = 2 from that in pure P123 micelles (n = 0). About 2.2 times increase in k_q values has been observed for C481 and C152 at n = 2 compared with that at n = 0. With SDS, the k_q value increases by a factor of about 1.6, 1.8, 1.9, and 1.4 for C153, C481, C152, and C151, respectively, at n = 2 from that in pure P123 micelle. There are two possibilities for the gradual increase in k_q values with the addition of ionic surfactant to P123 micellar solution. It could be the increased micropolarity due to enhanced hydration (as indicated from the marginal red shift of the coumarin spectra, cf. Figure 1) that will facilitate the ET reaction.[29] However, this argument should also hold for the addition of neutral surfactant, TX100, in P123 micellar solution, but for this system, we do not observe any increase in the k_q values. We thus feel that the extent of polarity change in the present system ($\Delta\varepsilon \approx 5$, cf. Figure 1) with the addition of surfactant is not enough for any significant change in the observed k_q values, and the observed changes in the k_q values in the presence of ionic surfactants are not directly related to the increased micropolarity. Besides the

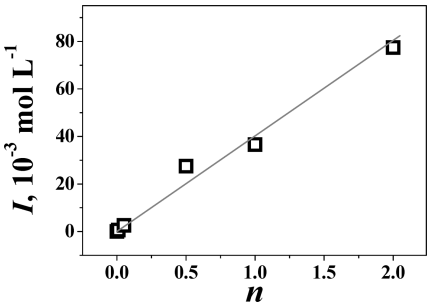

Figure 8. Ionic strength (I) versus n for P123−ionic surfactant (SDS and CTAC) systems. The line is just a guide to the eye.

small increase in micropolarity, the increased ionic strength in the Corona region due to the incorporation of ionic heads and counterions (with the addition of SDS and CTAC) will also favor ET reactions owing to the greater stabilization of the highly polar coumarin excited states and the transients produced on ET interaction.[29,91] Assuming full dissociation of ionic surfactants in P123−surfactant micellar aggregates, we have calculated the ionic strength, I ($= 1/2\sum_i C_i Z_i^2$, where C_i and Z_i are the concentration and valence (or oxidation) number of the ith species, respectively[91]), in the Corona region. Concentrations of ionic surfactants in the Corona region were calculated on the basis of the number of surfactant units in the Corona region of P123−surfactant systems. Correlation of I with n is shown in Figure 8. It has been found that the ionic strength too follows a linear correlation with n, as observed for the k_q values of P123−SDS and P123−CTAC systems. Comparing these results obtained with ionic and nonionic surfactants in P123 micelles, we can infer that it is the ionic strength over the micropolarity that governs the reaction dynamics in P123−surfactant micellar aggregates. However, the observed marginal decrease in k_q values with the addition of TX100 (at very high n values) is not yet clear. Besides, it should also be noted that the microviscosity and the free energy of the reaction should also be considered for a better perspective of the quenching rates, as discussed in the later sections.

At this juncture, it is interesting to compare the ET rates in the present P123−surfactant systems with that in pure micelles. Our ET studies for similar systems are previously reported in pure anionic (SDS[10]), cationic (CTAB[8]), and neutral (TX100,[7] P123,[13] F88[15]) micelles. Larger donor−acceptor separation in cationic micelles as a result of greater counterion condensation in the Stern layer[92,93] was attributed to the considerably slower quenching rates than those observed in anionic micelles, which is again lower than that in neutral micelles (with no counterion effect), $k_q^{TX100} \approx 1.7k_q^{SDS} \approx 11.1k_q^{CTAB}$ (for C153-DMAN systems).[7,8,10] Recently, similar observations were also made by Ghosh et al.[18] In the present P123−ionic surfactant micellar aggregates, however, we did not observe a decrease in ET rates as expected from the counterion effect, rather it increases in the presence of ionic surfactants, $k_q^{P123-CTAC(n=2)} \approx 1.3k_q^{P123-SDS(n=2)} \approx 2.1k_q^{P123(n=0)}$ ($\approx 2.4k_q^{P123-TX100(n=2)}$). The number density of ionic surfactants in copolymer−surfactant supramolecular assemblies is quite small compared with that in pure ionic micelles apart from the larger Corona thickness of the copolymer−surfactant supramolecular assemblies ($\geq$30 Å, cf. Table 4) compared with that of pure ionic micelles ($\sim$9 Å[8,10]). Both of these factors reduce the crowding of counterions and thus its negative influence on the ET rates in the copolymer−surfactant aggregates. Moreover, among the neutral copolymer

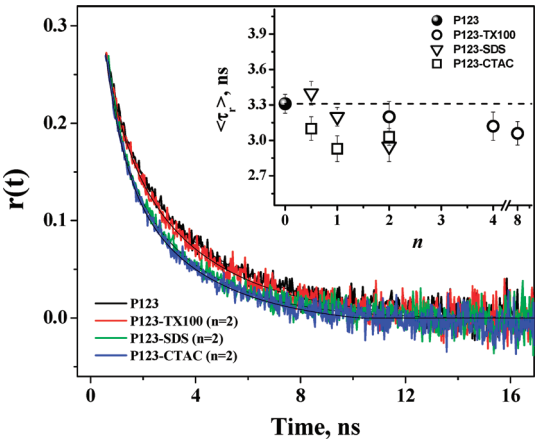

Figure 9. Fluorescence anisotropy decays of C153 in P123−surfactant micellar aggregates. Inset shows the variation in the average anisotropy decay time constant, $\langle\tau_r\rangle$, as a function of n in different P123−surfactant systems. Solid symbol represents the same in pure P123 micelle.

micelles (with different EO/PO ratios) ET rates were observed to be dependent on the degree of hydration in the corona region, $k_q^{F88(\varepsilon\approx 23)} \approx 2.9\ k_q^{P123(\varepsilon\approx 10)}$.[15] Hence, we believe that the increase in k_q value in P123−ionic surfactant aggregates is a direct consequence of reduced crowding of counterions along with increased ionic strength and hydration in the Corona region of aggregates. Therefore, copolymer−surfactant systems are better suited for a faster ET reaction undermining the inherent difficulties observed with pure ionic micelles.

To understand the solute microenvironment inside the P123−surfactant micellar aggregates, we carried out fluorescence anisotropy measurements of C153 in selected micellar media. In all of the P123−surfactant systems studied, the anisotropy decays were biexponential in nature (cf. Figure 9), an observation similar to those previously reported for other micellar systems.[13,94−98] The two rotational relaxation times as estimated for the present systems at different n values were around 0.7 ($\pm$0.2 ns) and 3.6 ns ($\pm$0.3 ns). The average rotational relaxation times $\langle\tau_r\rangle$ in the present systems were also calculated using the following relation

$$\langle\tau_r\rangle = a_{r1}\tau_{r1} + a_{r2}\tau_{r2} \qquad (11)$$

where τ_{r1} and τ_{r2} are the fast and slow rotational relaxation times and a_{r1} and a_{r2} are their relative contributions, respectively. In the present context, a detailed analysis of the anisotropy results following the rigorous two-step model,[13,94−96,99,100] as discussed in many micellar systems, is not essential because the average rotational relaxation times are sufficient to understand the kind of changes in the microviscosities in P123 micelle with the gradual addition of surfactants. Therefore, to correlate anisotropy results in different P123−surfactant systems, we simply used the $\langle\tau_r\rangle$ values estimated at different n values, shown in the inset of Figure 9. It is clearly indicated that in the presence of the surfactants, the microviscosity in the Corona region is only marginally reduced. Decrease in microviscosity with increase in n has also been observed by Mali et al.[94,101] Nevertheless, this negligible change is not expected to impart any significant influence on the translational diffusion of the reactants in the Corona region of the micelle and thus ET dynamics. It has been previously demonstrated that the micellar ET reaction occurs effectively under nondiffusive condition, that is with negligible influence from the translational diffusion of the reactants in the micellar phase.[10,13]

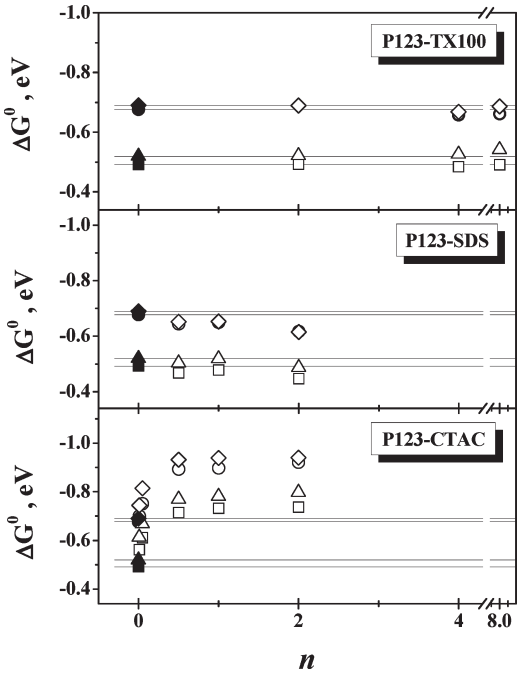

Figure 10. Variation in the free energy of ET reaction as a function on n in different P123−surfactant systems. Symbols are as given in the Figure 7 caption. Horizontal reference lines correspond to the respective dyes in pure P123 micelles.

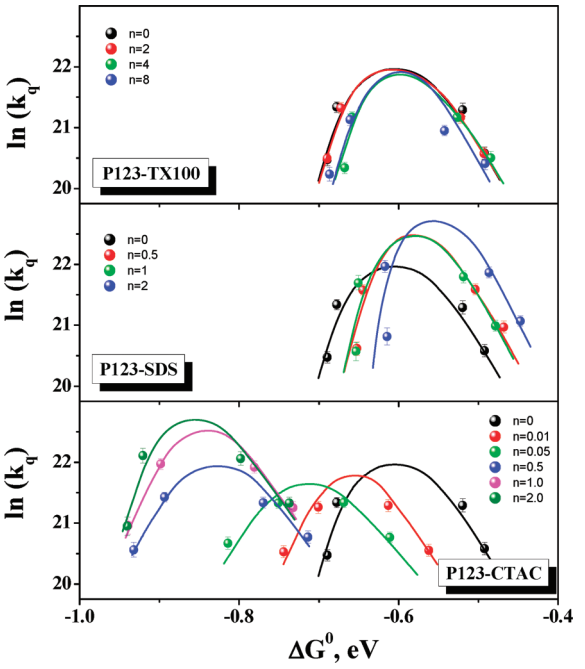

Figure 11. Plot of $\ln(k_q)$ versus ΔG^0 shows Marcus bell-shaped correlation for all P123−surfactant micellar aggregates. The solid lines are just a guide to the eyes. With the gradual increase in surfactant concentration in P123 micellar media, the appearance of Marcus inversion region shifts substantially on the exergonicity scale, toward higher or lower exergonicity, depending on the nature of cosurfactant used.

Significant changes in redox properties (up to ∼0.3 V) of coumarins and DMAN, depending on the nature of the surfactant used and the composition of P123−surfactant systems, are clearly indicated from redox potentials listed in Tables 1−3, except that the E_{00} energies for the coumarins remain almost similar in all P123−surfactant systems. To note, in our previous studies, we have observed an alteration in the reduction potential (by ∼0.1 V) of an anionic dye, C343, in P123 micelle by the addition of cationic surfactant CTAC (n = 0.2).[102] The electrostatic attraction of the oppositely charged dye and the surfactant headgroup leads to the gradual shifting of probe location from the micellar surface to the core−Corona interface of the P123−CTAC aggregates and thus change in the chemical environment of C343. However, to understand clearly the influence of cosurfactants on the ET dynamics and energetics, in the present case, we deliberately worked with neutral dyes to circumvent any special interaction of the dye with the surfactant head groups. To understand the influence of surfactants and their concentrations on the ET energetics in P123−surfactant systems, we tried to correlate the free energy changes for the ET reactions with the surfactant to copolymer ratio, as shown in Figure 10. The addition of TX100 to P123 solution does not alter the exergonicity ($-\Delta G^0$) of the reaction even at fairly high surfactant concentration (n = 8), in contrast with SDS or CTAC (n = 2). Among the ionic surfactants, SDS decreases the reaction exergonicity, whereas CTAC increases it, as expected from the redox potentials of the reactants. Furthermore, the extent of increase in the reaction exergonicity with CTAC is different above and below $n \approx 0.5$. A monotonic decrease in the exergonicity has been observed with SDS, although the extent is quite less compared with that with CTAC. These results emphasize the suitable selection of cosurfactant and their concentrations to be used to modulate or tune the exergonicity of ET reactions in P123−surfactant systems.

Because the interaction between coumarins and amine is known to be due to ET process,[7−10,13,18,19,103−106] it is interesting to see how the experimental quenching rates (k_q) correlate with the free-energy changes (ΔG^0) for the ET reactions. Correlations between the observed quenching constants (k_q) and the ΔG^0 values for different coumarin−amine pairs in all P123−surfactant micellar aggregates is shown in Figure 11. It is evident from Figure 11 that at low exergonicity ($-\Delta G^0$) the reaction rate increases with the exergonicity of the reaction, whereas at higher driving forces the rate decreases with the reaction exergonicity in all P123−surfactant systems.[29] The appearance of Marcus inversion is seen to occur at reasonably lower exergonicity because of the partial contribution of solvent reorganization energy,[6−10,13,18−21,29] owing to slower solvent reorganization in micelles[46,107−110] and envisaged on the basis of 2DET theory.[28] Present results provide an evidence of the predicted inversion from Marcus ET theory in any type of mixed micellar aggregates. To be noted, in general, the symmetric nature of the Marcus correlation is observed in micellar media because of the limited exergonicity scale covered for micellar ET reactions. In the present case also, the Marcus correlations shown in Figure 11 apparently seem to be symmetric in nature. The asymmetry in the Marcus correlation curves for ET reactions mainly arises at very high exergonicity region ($-\Delta G^0 \gg 1.0$ eV), where participation of the high-frequency vibrational modes enhances the observed ET rates. Because the maximum exergonicity covered in the present work is not that high ($-\Delta G^0$ <1 eV), we expect that there is no involvement of the high-frequency vibrational modes in the present systems studied. Accordingly, the symmetric nature of the Marcus correlation curves is quite expected, as indicated from Figure 11. The most interesting observation from the present study is that the Marcus inversion

region undergoes a gradual shift toward higher exergonicity by ~0.3 eV with an increase in the CTAC concentration, but with SDS, it shows a shift toward lower exergonicity by ~0.1 eV. No significant shift of Marcus correlation is observed with the addition of TX100. The hydrophilicity of ionic surfactants, for example, SDS and CTAC, is much higher than that of TX100. Moreover, solvation dynamics (determined by solvent diffusion, mainly confined water in the micelle) in the Stern layer of ionic micelles are much faster than those in the Palisade layer of TX100.[107] Therefore, the addition of ionic surfactants like CTAC and SDS in P123 micellar media is expected to shift the appearance of Marcus inversion by a greater extent than that with neutral surfactant TX100. Although, the extent of this shift even with the ionic surfactants (~0.3 eV) is smaller in comparison with that observed in previous studies by changing the nature of the micelles (~0.7 eV9), but it convincingly demonstrates the possibility of tuning reaction exergonicity by adding a cosurfactant in a single block copolymer micelle. The gradual shift of Marcus inversion toward higher exergonicity in the presence of CTAC indicates an increased contribution of solvent reorganization with increasing CTAC concentration, possibly due to faster solvation dynamics in the P123−CTAC system than in pure P123 micelle. The observation in the case of P123−SDS is just opposite to that in P123−CTAC system, and this needs further investigation to understand the reason behind it. However, a tentative reasoning for the above observation can be obtained from the reported solvation dynamic results on the similar systems, as discussed below.

In the recent solvent relaxation studies of coumarin 480 (C480) in P123−CTAC systems, Dey et al.[97] have reported that the observed Stokes' shift decreases from 1850 to 1600 cm^{-1} (with excitation near to the absorption maxima) on the addition of CTAC in P123 micelle. This indicates a faster solvation component in P123−CTAC aggregates than in pure P123 micelle (increased contribution of ultrafast component of Stokes' shift missed because of limited time resolution of the measurement). Hence, it is expected that the contribution of solvent reorganization will be more in P123−CTAC micellar aggregates than in pure P123 micelle and thus will shift the Marcus inversion region toward higher exergonicity. Following the report of Mandal et al.,[98] in the presence of SDS, the observed Stokes' shift for C480 increases from 1845 to 2040 cm^{-1} (with excitation near to the absorption maxima), indicating slower solvent reorganization dynamics in P123−SDS aggregates than in pure P123 micelle. Consequently, because of a relatively lower solvent reorganization, a shift of Marcus correlation toward lower exergonicity is expected. Therefore, the relative propensity of ET and solvation rate, responsible for the contribution of solvent reorganization energy and thus the appearance of inversion region, varies with the nature and composition of the copolymer−surfactant aggregates. Apart from the shift of Marcus correlation along the exergonicity scale, there is also a substantial increase in the reaction rate in the P123−ionic surfactant supramolecular aggregates (cf. Figure 7). Hence, the present results suggest the possibility of modulation of ET reactions not only in the appearance of Marcus inversion along the exergonicity scale but also to tune the ET rates substantially by modulating the micellar environment with a relatively more hydrophilic ionic cosurfactant.

CONCLUSIONS

From the present study of photoinduced bimolecular ET dynamics between various 7-aminocoumarin derivatives and DMAN in copolymer−surfactant aggregates prepared in aqueous 1% P123 triblock copolymer micellar solution with varying concentration of TX100, SDS, and CTAC, it is indicated that there is a possibility of tuning the reaction exergonicity as well as the ET rate by using ionic surfactants in combination with a triblock copolymer micelle. Similar to other micellar media, copolymer−surfactant supramolecular aggregates also exhibit Marcus inversion behavior for bimolecular photoinduced ET reactions. The increase in the ET rates in P123−ionic surfactant micelles has been correlated with the increase in the ionic strength because of the incorporation of ionic heads and counterions in the Corona region with an increase in ***n***. Alteration in the redox potentials were observed to modify the reaction exergonicity, and depending on the relative propensity of ET and solvation rates, the appearance of inversion in ET rates shifts along the exergonicity scale.

AUTHOR INFORMATION

Corresponding Author

*E-mail: manojk@barc.gov.in, manojbarc@yahoo.co.in. Fax: 91-22-25505151/25519613.

ACKNOWLEDGMENT

Encouragement and support from Dr. T. Mukherjee, Director, Chemistry Group, BARC, and Dr. S. K. Sarkar, Head, RPC Division, BARC, are gratefully acknowledged. S.D. acknowledges the Indian Science Academies for his Summer Research Fellowship.

REFERENCES

(1) Swallen, S. F.; Weidemaier, K.; Fayer, M. D. *J. Phys. Chem.* **1995**, *99*, 1856.
(2) Swallen, S. F.; Weidemaier, K.; Tavernier, H. L.; Fayer, M. D. *J. Phys. Chem.* **1996**, *100*, 8106.
(3) Tavernier, H. L.; Laine, F.; Fayer, M. D. *J. Phys. Chem. A* **2001**, *105*, 8944.
(4) Pal, S. K.; Mandal, D.; Sukul, D.; Bhattacharyya, K. *Chem. Phys.* **1999**, *249*, 63.
(5) Fukuzumi, S.; Nishimine, M.; Ohkubo, K.; Tkachenko, N. V.; Lemmetyinen, H. *J. Phys. Chem. B* **2003**, *107*, 12511.
(6) Kumbhakar, M.; Nath, S.; Mukherjee, T.; Pal, H. *J. Chem. Phys.* **2005**, *122*, 084512.
(7) Kumbhakar, M.; Nath, S.; Mukherjee, T.; Pal, H. *J. Chem. Phys.* **2004**, *120*, 2824.
(8) Kumbhakar, M.; Nath, S.; Mukherjee, T.; Pal, H. *J. Chem. Phys.* **2005**, *123*, 034705.
(9) Kumbhakar, M.; Singh, P. K.; Nath, S.; Bhasikuttan, A. C.; Pal, H. *J. Phys. Chem. B* **2008**, *112*, 6646.
(10) Kumbhakar, M.; Nath, S.; Pal, H.; Sapre, A. V.; Mukherjee, T. *J. Chem. Phys.* **2003**, *119*, 388.
(11) Kumbhakar, M.; Singh, P. K.; Nath, S.; Satpati, A. K.; Pal, H. *J. Phys. Chem. B* **2010**, *114*, 10057.
(12) Kumbhakar, M.; Mukherjee, T.; Pal, H. *Chem. Phys. Lett.* **2005**, *410*, 94.
(13) Satpati, A. K.; Kumbhakar, M.; Nath, S.; Pal, H. *J. Phys. Chem. B* **2007**, *111*, 7550.
(14) Satpati, A. K.; Kumbhakar, M.; Nath, S.; Pal, H. *J. Photochem. Photobiol., A* **2008**, *200*, 270.
(15) Verma, P.; Nath, S.; Singh, P. K.; Kumbhakar, M.; Pal, H. *J. Phys. Chem. B* **2008**, *112*, 6363.
(16) Mukherjee, T. K.; Mishra, P. P.; Datta, A. *Chem. Phys. Lett.* **2005**, *407*, 119.
(17) Mandal, U.; Ghosh, S.; Dey, S.; Adhikari, A.; Bhattacharyya, K. *J. Chem. Phys.* **2008**, *128*, 164505.

(18) Ghosh, S.; Mondal, S. K.; Sahu, K.; Bhattacharyya, K. *J. Chem. Phys.* **2007**, *126*, 204708.
(19) Ghosh, S.; Sahu, K.; Mondal, S. K.; Sen, P.; Bhattacharyya, K. *J. Chem. Phys.* **2006**, *125*, 54509.
(20) Chakraborty, A.; Chakrabarty, D.; Hazra, P.; Seth, D.; Sarkar, N. *Chem. Phys. Lett* **2003**, *382*, 508.
(21) Chakraborty, A.; Chakrabarty, D.; Hazra, P.; Seth, D.; Sarkar, N. *Chem. Phys. Lett.* **2004**, *387*, 517.
(22) Chakraborty, A.; Seth, D.; Seth, P.; Sarkar, N. *J. Phys. Chem. B.* **2006**, *110*, 16607.
(23) Chakraborty, A.; Seth, D.; Setua, P.; Sarkar, N. *J. Chem. Phys.* **2006**, *124*, 074512.
(24) Chakraborty, A.; Seth, D.; Setua, P.; Sarkar, N. *J. Chem. Phys.* **2008**, *128*, 204510.
(25) Chen, L.; Wood, P. D.; Mnyusiwalla, A.; Marlinga, J.; Johnston, L. J. *J. Phys. Chem. B* **2001**, *105*, 10927.
(26) Singh, A. K.; Mondal, J. A.; Ramakrishna, G.; Ghosh, H. N.; Bandyopadhyay, T.; Palit, D. K. *J. Phys. Chem. B* **2005**, *109*, 4014.
(27) Glusac, K.; Goun, A.; Fayer, M. D. *J. Chem. Phys.* **2006**, *125*, 054712.
(28) Sumi, H.; Marcus, R. A. *J. Chem. Phys.* **1986**, *84*, 4894.
(29) Kavarnos, G. J. *Fundamentals of Photoinduced Electron Transfer*; VCH Publishers: New York, 1993.
(30) Lakowicz, J. R. *Principle of Fluorescence Spectroscopy*, 3rd ed.; Spinger: New York, 2006.
(31) Yoshihara, K.; Tominaga, K.; Nagasawa, Y. *Bull. Chem. Soc. Jpn.* **1995**, *68*, 696.
(32) Kumbhakar, M.; Nath, S.; Mukherjee, T.; Pal, H. *J. Indian Chem. Soc.* **2010**, *87*, 173.
(33) Kumbhakar, M.; Goel, T.; Mukherjee, T.; Pal, H. *J. Phys. Chem. B* **2005**, *109*, 14168.
(34) Kumbhakar, M.; Goel, T.; Mukherjee, T.; Pal, H. *J. Phys. Chem. B* **2005**, *109*, 18528.
(35) Charlton, I. D.; Doherty, A. P. *J. Phys. Chem. B* **2000**, *104*, 8327.
(36) Molina-Bolivar, J. A.; Aguiar, J.; Ruiz, C. C. *J. Phys. Chem. B* **2002**, *106*, 870.
(37) Philies, J. D.; Hunt, R. H.; Strang, K.; Sushkin, N. *Langnuir* **1995**, *11*, 3408.
(38) Dutt, G. B. *J. Phys. Chem. B* **2003**, *107*, 3131.
(39) Kumbhakar, M.; Ganguly, R. *J Phys. Chem. B.* **2007**, *111*, 3935.
(40) Ganguly, R.; Aswal, V. K. *J. Phys. Chem. B* **2008**, *112*, 7726.
(41) Charlton, I. D.; Doherty, A. P. *J. Phys. Chem. B* **1999**, *103*, 5081.
(42) Charlton, I. D.; Doherty, A. P. *Anal. Chem.* **2000**, *72*, 687.
(43) Bendedouch, D.; Chen, S.-H. *J. Phys. Chem.* **1984**, *88*, 648.
(44) Kalyanasundaram, K.; Gratzel, M.; Thomas, J. K. *J. Am. Chem. Soc.* **1975**, *97*, 3915.
(45) Dutt, G. B. *J. Phys. Chem. B* **2002**, *106*, 7398.
(46) Kumbhakar, M.; Goel, T.; Mukherjee, T.; Pal, H. *J. Phys. Chem. B* **2004**, *108*, 19246.
(47) Streletzky, K.; Philies, J. D. *Langnuir* **1995**, *11*, 42.
(48) Kalyansundaram, K. *Photochemistry in Microheterogeneous Systems*; Academic Press: Orlando, FL, 1987.
(49) Chu, B.; Zhou, Z. Physical Chemistry of Polyoxyalkylene Block Copolymer Surfactants. In *Nonionic Surfactants*; Nace, V. M., Ed.; Surfactant Science Series; Marcel Dekker: New York, 1996; Vol. 60, p 67.
(50) Ganguly, R.; Kumbhakar, M.; Aswal, V. K. *J. Phys. Chem. B* **2009**, *113*, 9441.
(51) Hara, K.; Kuwabara, H.; Kajimoto, O. *J. Phys. Chem. A.* **2001**, *105*, 7174.
(52) Hara, K.; Baden, N.; Kajimoto, O. *J. Phys.: Condens. Matter* **2004**, *16*, S1207.
(53) Hara, K.; Ito, N.; Kuwabara, H.; Kajimoto, O. *High Pressure Res.* **2002**, *22*, 515.
(54) Molotsky, T.; Koifman, N.; Huppert, D. *J. Phys. Chem. A* **2002**, *106*, 12185.
(55) Kumbhakar, M. *J. Phys. Chem. B* **2007**, *111*, 14250.
(56) Kumbhakar, M. *J. Phys. Chem. B* **2007**, *111*, 12154.
(57) Ganguly, R.; Aswal, V. K.; Hassan, P. A.; Gopalakrishnan, I. K.; Kulshreshtha, S. K. *J. Phys. Chem. B* **2006**, *110*, 9843.
(58) Chen, D.; Li, Z.; Yu, C.; Shi, Y.; Zhang, Z.; Tu, B.; Zhao, D. *Chem. Mater.* **2005**, 17.
(59) Tan, Y.; Srinivasan, S.; Choi, K.-S. *J. Am. Chem. Soc.* **2005**, *127*, 3596.
(60) Bronich, T. K.; Ouyang, M.; Kabanov, V. A.; A. F. C. S., J. E.; Kabanov, A. V. *J. Am. Chem. Soc.* **2002**, *124*, 11872.
(61) Thurn, T.; Couderc, S.; Sidhu, J.; Bloor, D. M.; Penfold, J.; Holzwarth, J. F.; Wyn-Jones, E. *Langmuir* **2002**, *18*, 9267.
(62) Vieira, J. B.; Thomas, R. K.; Li, Z. X.; Penfold, J. *Langmuir* **2005**, *21*, 4441.
(63) Couderc, S.; Li, Y.; Bloor, D. M.; Holzwarth, J. F.; Wyn-Jones, E. *Langmuir* **2001**, *17*, 4818.
(64) Lof, D.; Tomsic, M.; Glatter, O.; Fritz-Popovski, G.; Schillen, K. *J. Phys. Chem. B* **2009**, *113*, 5478.
(65) Almgren, M.; Stam, J. V.; Lindblad, C.; Li, P.; Stilbs, P.; Bahadur, P. *J. Phys. Chem.* **1991**, *95*, 5677.
(66) Hecht, E.; Mortensen, K.; Gradzielski, M.; Hoffman, H. *J. Phys. Chem.* **1995**, *99*, 4866.
(67) Li, Y.; Xu, R.; Couderc, S.; Bloor, D. M.; Holzwarth, J. F.; Wyn-Jones, E. *Langmuir* **2001**, *17*, 5742.
(68) Lisi, R. D.; Lazzara, G.; Milioto, S.; Muratore, N. *J. Phys. Chem. B* **2004**, *108*, 18214.
(69) Silva, R. C. D.; Olofsson, G.; Schillen, K.; Loh, W. *J. Phys. Chem. B* **2002**, *106*, 1239.
(70) Tapia, M. J.; Burrows, H. D.; Valente, A. J. M.; Pradhan, S.; Scherf, U.; Lobo, V. M. M.; Pina, J.; Melo, J. S. D. *J. Phys. Chem. B* **2005**, *109*, 19108.
(71) Couderc-Azouani, S.; Sidhu, J.; Thurn, T.; Xu, R.; Bloor, D. M.; Penfold, J.; Holzwarth, J. F.; Wyn-Jones, E. *Langmuir* **2005**, *21*, 10197.
(72) Jansson, J.; Schillen, K.; Nilsson, M.; Soderman, O.; Fritz, G.; Bergmann, A.; Glatter, O. *J. Phys. Chem. B* **2005**, *109*, 7073.
(73) Jansson, J.; Schillen, K.; Olofsson, G.; Silva, R. C. D.; Loh, W. *J. Phys. Chem. B* **2004**, *108*, 82.
(74) Vangeyte, P.; Leyh, B.; Auvray, L.; Grandjean, J.; Misselyn-Bauduin, A.-M.; Jerome, R. *Langmuir* **2004**, *20*, 9019.
(75) Li, Y.; Xu, R.; Bloor, D. M.; Holzwarth, J. F.; Wyn-Jones, E. *Langmuir* **2000**, *16*, 10515.
(76) Lof, D.; Niemiec, A.; Schillen, K.; Loh, W.; Olofsson, G. *J. Phys. Chem. B* **2007**, *111*, 5911.
(77) Lof, D.; Schillen, K.; Torres, M. F.; Muller, A. J. *Langmuir* **2007**, *23*, 11000.
(78) Zheng, Y.; Davis, H. T. *Langmuir* **2000**, *16*, 6453.
(79) O'Connor, D. V.; Phillips, D. *Time Correlated Single Photon Counting*; Academic Press: New York, 1984.
(80) Rehm, D.; Weller, A. *Israel J. Chem.* **1970**, *8*, 259.
(81) Pal, H.; Nad, S.; Kumbhakar, M. *J. Chem. Phys.* **2003**, *119*, 443.
(82) Brown, J. C.; Pusey, P. N.; Dietz, R. J. *J. Chem. Phys.* **1975**, *62*, 1136.
(83) Hassan, P. A.; Kulshreshtha, S. K. *J. Colloid Interface Sci.* **2006**, *300*, 744.
(84) Aswal, V. K.; Goyal, P. S. *Curr. Sci.* **2000**, *79*, 947.
(85) Pedersen, J. S. *Adv. Colloid Interface Sci.* **1997**, 171.
(86) Aswal, V. K.; Goyal, P. S.; Thiyagarajan, P. *J. Phys. Chem.* **1998**, *102*, 2469.
(87) Kumbhakar, M.; Nath, S.; Rath, M. C.; Mukherjee, T.; Pal, H. *Photochem. Photobiol.* **2004**, *79*, 1.
(88) Rohatgi-Mukherjee, K. K. *Fundamentals of Photochemistry*; New Age International: New Delhi, India, 1986.
(89) Ganguly, R.; Aswal, V. K.; Hassan, P. A. *J. Collod. Interface Sci.* **2007**, *315*, 693.
(90) Li, Y.; Xu, R.; Couderc, S.; Bloor, D. M.; Holzwarth, J. F.; Wyn-Jones, E. *Langmuir* **2001**, *17*, 183.
(91) Atkins, P. W.; Paula, J. d. *Atkin's Physical Chemistry*, 8th ed.; Oxford University Press: Oxford, U.K., 1994.
(92) Berr, S. *J. Phys. Chem.* **1987**, *91*, 4760.
(93) Berr, S.; Jones, R. R. M.; Johnson, J. J. S. *J. Phys. Chem.* **1992**, *96*, 5611.

(94) Mali, K. S.; Dutt, G. B.; Mukherjee, T. *J. Phys. Chem. B* **2007**, *111*, 5878.
(95) Maiti, N. C.; Krishna, M. M. G.; Britto, P. J.; Periasamy, N. *J. Phys. Chem. B.* **1997**, *101*, 11051.
(96) Quitevis, E. L.; Marcus, A. H.; Fayer, M. D. *J. Phys. Chem.* **1993**, *97*, 5762.
(97) Dey, S.; Adhikari, A.; Mandal, U.; Ghosh, S.; Bhattacharyya, K. *J. Phys. Chem. B* **2008**, *112*, 5020.
(98) Mandal, U.; Adhikari, A.; Dey, S.; Ghosh, S.; Mondal, S. K.; Bhattacharyya, K. *J. Phys. Chem. B* **2007**, *111*, 5896.
(99) Lipari, G.; Szabo, A. *Biophys. J.* **1980**, *30*, 489.
(100) Lipari, G.; Szabo, A. *J. Am. Chem. Soc.* **1982**, *104*, 4546.
(101) Mali, K. S.; Dutt, G. B.; Mukherjee, T. *J. Chem. Phys.* **2007**, *127*, 154904.
(102) Singh, P. K.; Satpati, A. K.; Kumbhakar, M.; Pal, H.; Nath, S. *J. Phys. Chem. B* **2008**, *112*, 11447.
(103) Shirota, H.; Pal, H.; Tominaga, K.; Yoshihara, K. *J. Phys. Chem. A* **1998**, *102*, 3089.
(104) Shirota, H.; Pal, H.; Tominaga, K.; Yoshihara, K. *Chem. Phys.* **1998**, *236*, 355.
(105) Pal, H.; Nagasawa, Y.; Tominaga, K.; Yoshihara, K. *J. Phys. Chem.* **1996**, *100*, 11964.
(106) Castner, E. W.; Kennedy, D.; Cave, R. J. *J. Phys. Chem. A* **2000**, *104*, 2869.
(107) Nandi, N.; Bhattacharyya, K.; Bagchi, B. *Chem. Rev.* **2000**, *100*, 2013.
(108) Tamoto, Y.; Segawa, H.; Shirota, H. *Langmuir* **2005**, *21*, 3757.
(109) (a) Shirota, H.; Segawa, H. *J. Phys. Chem. A* **2003**, *107*, 3719. (b) Shirota, H.; Tamoto, Y.; Segawa, H. *J. Phys. Chem. A* **2004**, *108*, 3244.
(110) Sarkar, N.; Datta, A.; Das, S.; Bhattacharyya, K. *J. Phys. Chem.* **1996**, *100*, 15483.